BRIEF COMMUNICATION



Carotid foramen size in the human skull tracks developmental changes in cerebral blood flow and brain metabolism

Arianna R. Harrington¹ | Christopher W. Kuzawa² | Doug M. Boyer¹

Correspondence

Arianna R. Harrington, Department of Evolutionary Anthropology, Duke University, Box 90383, Durham, NC 27708. Email: arianna.harrington@duke.edu

Abstract

Objectives: In humans, neuronal processes related to brain development elevate the metabolic rate of brain tissue relative to the body during early childhood. This phenomenon has been hypothesized to contribute to slow somatic growth in preadolescent *Homo sapiens*. The uncoupling of the brain's metabolic rate from brain size during development complicates the study of the evolutionary emergence of these traits in the fossil record. Here, we extend a method previously developed to predict interspecific differences in cerebral blood flow (a correlate of cerebral glucose use) to predict ontogenetic changes in human brain metabolism.

Materials and methods: Radii of the carotid foramen from an ontogenetic series of modern human crania were used to predict blood flow rates through the internal carotid arteries (ICA), which were compared to empirically measured ICA flow and brain metabolism values.

Results: Predictions of both absolute ICA blood flow rates and perfusion (ICA blood flow rates relative to brain size) generally match measured values in infancy and childhood. Maximum predicted ICA blood flow rates and perfusion were found to occur between ages 5 and 8, which roughly correspond to the age of maximum measured ICA blood flow rate and absolute and brain mass-specific rate of whole brain glucose uptake.

Discussion: These findings suggest that, during human growth and development, the size of the carotid foramen corresponds well to blood flow requirements through the ICA, and the method tested here may provide new opportunities for studying developmental changes in brain metabolism using osteological samples, including fossil hominins.

KEYWORDS

blood flow rate, carotid foramen, energetics, human life history evolution, internal carotid artery, perfusion

1 | INTRODUCTION

1.1 | Background

The unusually high energy requirements of the human brain have long been of interest to anthropologists (Armstrong, 1983; Isler & van Schaik, 2006; Martin, 1981). In human adults, the brain accounts for 20% of the body's resting metabolic expenditure. This figure appears to be much higher than in most mammals (Kuzawa, 1998) and is thought to have required energetic tradeoffs with other functions to achieve (Aiello & Wheeler, 1995; Isler & van Schaik, 2009; Leonard & Robertson, 1992). Although these costs are important across the lifecycle, the energetic demands of the brain are recognized as being especially high early in life

(Foley & Lee, 1991). Recent work using brain imaging data showed that human brain metabolism accounts for a lifetime peak of 66% of resting metabolic rate at 4–5 years of age (Kuzawa et al., 2014). This analysis also revealed evidence for a strong inverse linear relationship between metrics of brain energetics and body weight growth rate between infancy and puberty, consistent with the hypothesis that high brain energy requirements required a compensatory reduction in expenditure on somatic growth (Kuzawa et al., 2014). Thus, the required deferment of major somatic growth costs results in a defining feature of human development: unusually slow growth during childhood followed by a pubertal growth spurt (Walker, Hill, Burger, & Hurtado, 2006). Because the peak in brain energetics occurs after the age of complete weaning,

¹Department of Evolutionary Anthropology, Duke University, Durham, North Carolina

²Department of Anthropology, Northwestern University, Evanston, Illinois

and when onboard energy reserves (body fat) are at a lifetime nadir, this finding also supports the hypothesis that a social strategy of buffering via food sharing and cooperative care was likely a prerequisite for the evolution of the human brain (Isler & van Schaik, 2009).

Because energetically costly brain development coevolved with a suite of life history traits that characterize our species, reconstructing brain developmental energetics in fossil hominin samples would provide a means of probing the evolutionary emergence of these traits. However, whether it is possible to reconstruct developmental brain costs from the fossil record is an open question. Past work, primarily in adult interspecific samples, has generally inferred brain energetic costs from brain size (Armstrong, 1983; de León et al., 2008; Hofman, 1983; Isler & van Schaik, 2006; McNab & Eisenberg, 1989). All these studies implicitly or explicitly rely on the assumption that metabolic expenditure per unit of brain volume or mass is constant across species. There is considerable evidence that this assumption is not met for interspecific samples (Karbowski, 2007) or for intraspecific samples during development (Chugani, Phelps, & Mazziotta, 1987). Karbowski (2007) showed that smaller brained species tended to have more energy dense brains and Kuzawa et al. (2014) showed that per-gram brain metabolic rates change ontogenetically in humans. In humans, the rate of glucose use per gram of brain tissue rises by a factor of 2.5 between birth and 4 years of age as synaptic densities and related energy-intensive processes increase (Figure 1a, b; Kuzawa et al., 2014).

One approach to estimating brain metabolic rates is to examine the rate of cerebral blood flow, which has been shown to be a strong correlate of the rates of glucose and oxygen utilization in the brain (Hawkins, Mans, Davis, Hibbard, & Lu, 1983; Lou, Edvinsson, & MacKenzie, 1987; Willie, Tzeng, Fisher, & Ainslie, 2014). Recently, Seymour, Angove, Snelling, and Cassey (2015) and Seymour, Bosiocic, and Snelling (2016) presented a method to predict blood flow rate through the cranial foramina that transmit the arteries supplying the brain, making it possible to infer brain metabolism independently of endocranial volume in osteological samples. Specifically, they predicted rates of blood flow through the internal carotid artery (ICA) using the radius of the carotid foramen. The ICA is a branch of the common carotid artery and travels to the brain via a carotid foramen or canal in many mammals (Gillilan, 1972), where it primarily supplies cerebral structures (Coceani & Gloor, 1966; Tatu, Moulin, Bogousslavsky, & Duvernoy, 1998). Although the brain is also supplied by the vertebral arteries, which fuse to form the basilar artery and primarily supply hindbrain structures (Tatu, Moulin, Bogousslavsky, & Duvernoy, 1996), the majority of blood supply to the human brain is provided by the ICAs (Scheel, Ruge, & Schöning, 2000; Schöning & Hartig, 1998). Thus, the ability to predict ICA blood flow rate from the carotid foramen has been argued to be a powerful tool for inferring brain metabolic rates in extant and extinct hominins independent of brain size (Seymour et al., 2016; Seymour, Bosiocic, & Snelling, 2017).

Seymour et al. (2015) predicted the scaling relationships of ICA blood flow rate to brain mass in haplorhine primates and marsupials, as well as a sample of fossil hominins (Seymour et al., 2016; Seymour et al., 2017), and suggest that interlineage differences in the scaling exponents may reflect differences in cortical composition and cognitive

complexity. Although the methods and findings of Seymour et al. (2015, 2016, 2017) are provocative, it is often difficult to test whether the resulting predicted blood flow rates of the ICAs closely match in vivo, empirically measured values, as comparative data for ICA blood flow rates do not exist for many extant taxa, and never will for extinct ones. However, assessing whether there is a general concordance between measured and predicted values in species for which both are available is an important first step. Errors may be compounded because some of the variables that are used to predict ICA blood flow rates in Seymour et al.'s (2015) method are themselves estimated or predicted parameters (Boyer & Harrington, 2018a; Boyer & Harrington, in press).

Fortunately, data on ICA blood flow rates measured by color duplex sonography exist for humans of different ages (Kehrer & Schöning, 2009; Scheel et al., 2000; Schöning & Hartig, 1996). At the same time, limited data indicate that the diameter of the carotid foramen increases with age during childhood (Lang, Schafhauser, & Hoffmann, 1983). This makes it possible to predict ICA blood flow rates from carotid foramen size at different ages in humans and to compare these estimates to empirical blood flow values measured by ultrasound sonography.

1.2 | Study aims

In this article, we first aim to test the hypothesis that blood flow rate through the ICAs can be reliably predicted from the radius of its associated bony carotid foramen using the methods developed by Seymour et al. (2015). If predicted ICA blood flow rate values match measured ICA blood flow values reasonably well, this would support the utility of this method for estimating cerebral blood flow.

As another aim, we also test the hypothesis that developmental differences in carotid foramen size across samples varying in age, and hence age changes in ICA size, are correlated to previously reported age changes in the metabolic rate of the developing human brain. Previous studies of brain glucose use (Kuzawa et al., 2014) and cerebral blood flow (Kehrer & Schöning, 2009; Schöning & Hartig, 1996; Wu et al., 2016) reveal evidence for similar patterns of developmental change in these two measures, with both absolute metabolism and per-gram measures of metabolism rising during infancy and reaching peak values around 4-5 years of age, before gradually declining to adult levels. In addition, during human development, the pattern of change in whole brain glucose metabolism as a percentage of the body's resting metabolic rate corresponds to the pattern of change in whole brain glucose metabolism per gram of brain tissue (Figure 1c). This correspondence suggests that even in the absence of osteologically based estimates of body size or whole body metabolism, it may be possible to use measures of brain perfusion (rate of blood flow/brain mass) at different ages to identify developmental peaks in energy usage by the brain relative to the body. Here, we predicted that the ontogenetic pattern of change in perfusion of carotid foramen size would match the known ontogenetic change in mass-specific brain glucose use (brain glucose utilization rate/brain mass). Positive ontogenetic results would indicate this method is useful for probing developmental changes in the metabolic costs, and associated tradeoffs, of brain development in skeletal samples.

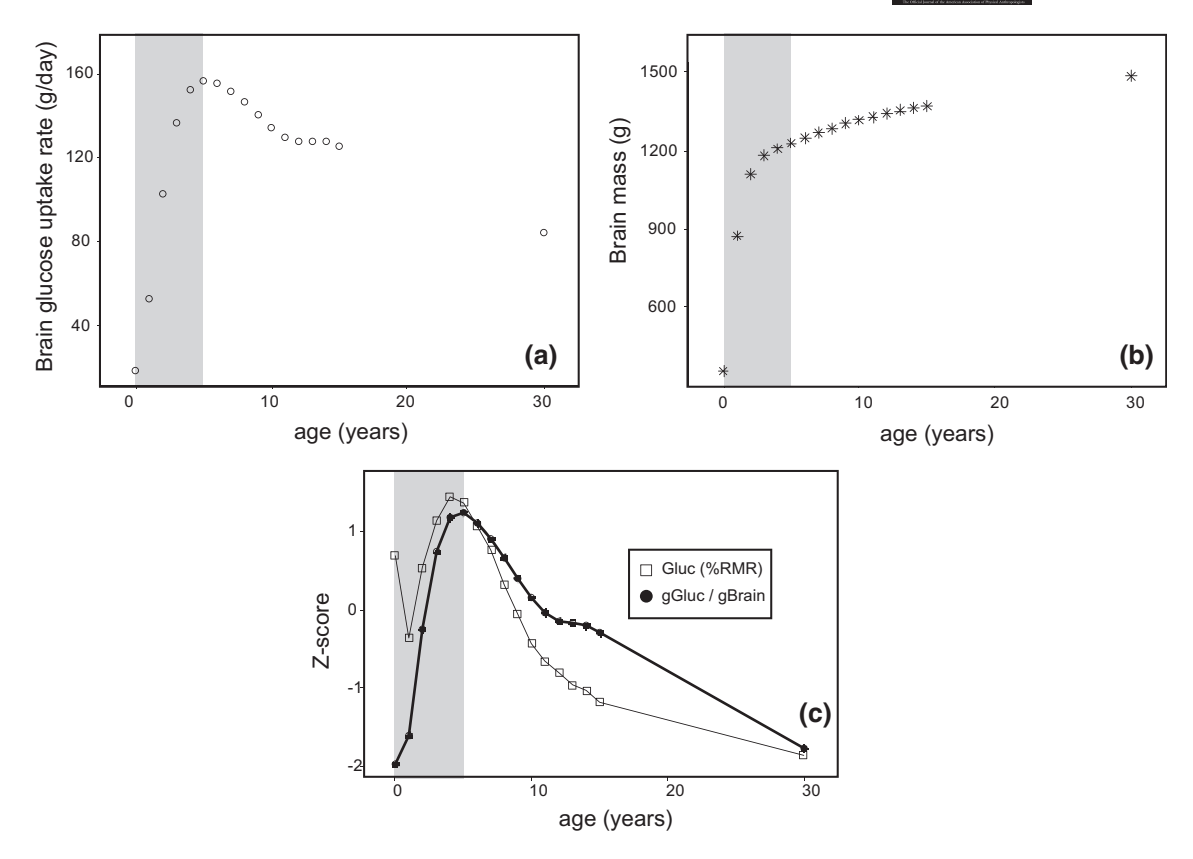


FIGURE 1 Age changes in (a) whole brain metabolic rate and (b) brain mass, illustrating the decoupling of the brain's energy costs from changes in brain size during human development. (c) Standardized Z-scores of whole brain glucose usage as a percentage of RMR (Gluc %RMR) and grams of glucose utilized by the brain as a proportion of brain mass (gGluc/gBrain) show correspondence in the timing of their peaks, illustrating that the gGluc/gBrain may be informative for assessing the timing of changes in Gluc %RMR in the absence of estimates of body metabolic rates. Brain glucose utilization rates, brain masses, and Gluc %RMR are mean values of males and females from Supporting Information, Tables S1 and S2 of Kuzawa et al. (2014); gray shaded areas represent values in the 0–5 years age range

2 | MATERIALS AND METHODS

All variables and abbreviations defined below are additionally listed and defined in Table 1. R code and data files used in the workflow described below are provided in Supporting Information.

Predicted blood flow rate through the internal carotid arteries $(Q_p$, in cm³/s) was calculated for humans of various ages, largely following the procedures of Seymour et al. (2015). The basis of their methods is a modified form of the Poiseuille–Hagan equation,

$$Q = \frac{\left(\tau \pi r^3\right)}{4\eta} \tag{1}$$

where Q = blood flow rate (cm³/s), τ = vessel wall shear stress (dyne / cm²), r = lumen radius of the vessel (cm), and η = blood viscosity (dyne s/cm). Although η can be considered interspecifically constant (Seymour et al., 2015), τ and r are variables that must be provided to solve for Q.

Vessel lumen radius (r) is estimated from the radius of the carotid foramen. Assuming that the ICA completely occupies the carotid canal and that ICA (wall thickness/lumen radius) = 0.4, Seymour et al. (2015) calculated the predicted ICA lumen radius (r_p) with the following equation:

$$r_p$$
 = (carotid foramen radius/1.4) (2)

In this study, external diameters of the carotid foramen for juvenile humans were collected from Lang et al. (1983), who reported measurements of various basicranial foramina in a sample of 98 infant and juvenile crania from the Institute of Anatomy of the Medical University of Innsbruck and the Institute of Anatomy of the University of Würzburg. Measurements and samples are reproduced in Supporting Information, Table S1. The same-side maximum and minimum diameters of the carotid foramen were averaged, then halved, to calculate a mean foramen radius for that side. The carotid canal foramen radius was then converted to $r_{\rm p}$ using Equation 2 (Table 2).

Wall shear stress (τ) is the friction experienced by blood and the endothelial lining of vessels (Cheng et al., 2007). In humans, τ has been found to differ by artery (Cheng et al., 2007; Wu et al., 2004) and by age in the same artery (Samijo et al., 1998). τ has also been found to vary interspecifically in the aorta (Greve et al., 2006; Weinberg & Ethier, 2007). However, when it comes to the ICA, it is not known exactly how τ varies inter- or intraspecifically. This prompted Seymour et al. (2015) to build a predictive model relating wall shear stress of the ICA ($\tau_{\rm ICA}$) to body mass ($M_{\rm b}$). $\tau_{\rm ICA}$ is first calculated using empirically measured radius ($r_{\rm ICA}$) and blood flow rates of the ICA ($Q_{\rm ICA}$) using the equation,

$$\tau = \frac{Q4\eta}{\pi r^3} \tag{3}$$

Although mean and peak values of τ_{ICA} have been reported for adults (Cebral, Castro, Putman, & Alperin, 2008), to our knowledge, there are no data on how this parameter changes with age in humans.

TABLE 1 Variables and abbreviations used in text

Term	Definition
ICA	Internal carotid artery, a branch of the carotid artery that enters the endocranium via the carotid foramen/canal to supply the brain in humans and many mammals
BGU	Whole brain glucose utilization rate, measured in grams of glucose/day
Perfusion	= rate of blood flow/100 g of brain mass
Mass-specific BGU	= BGU/100 g of brain mass
Q	Blood flow rate, sometimes referred to as flow volume by previous studies, measured in cm ³ /s
Q_{ICA}	Blood flow rate through the ICAs empirically measured by previous studies using ultrasound sonography techniques
Q_p	Blood flow rate through the ICAs predicted by this study using Equation 1
Total Q _{ICA}	= $2 \times Q_{\text{ICA}}$, representing measured bilateral blood flow through the ICAs
Total Q _p	= right $Q_{\rm p}$ + left $Q_{\rm p}$, representing predicted bilateral blood flow through the ICAs
r	Lumen radius of artery
r _{ICA}	Lumen radius of the ICA measured by previous studies from ultrasound sonography images
r _p	Lumen radius of the ICA estimated by this study from carotid foramen radii using Equation 2
τ	Vessel wall shear stress, measured in dyne/cm ²
$ au_{ICA}$	"Measured" wall shear stress of the ICA estimated from Equation 3 using $r_{\rm ICA}$ and $M_{\rm b}$
$ au_{p}$	Wall shear stress of the ICA predicted from Equation 4
η	Blood viscosity in dyne s/cm. Assumed to be constant at 0.04 dyne s/cm for mammals.
$M_{\rm b}$	Body mass, measured in kg

To model ontogenetic changes in τ_{ICA} , empirically measured mean Q_{ICA} and r_{ICA} of different age bins (Supporting Information, Table S2) were applied to Equation 3. The resulting τ_{ICA} values were regressed against M_b (Supporting Information, Figure S1) and a linear model was fit to the data, yielding the following equation:

$$\tau_p = 0.35 \times M_b - 40(p < 0.0001, r^2 = 0.75)$$
 (4)

Values for $\tau_{\rm p}$ (predicted from Equation 4) and $r_{\rm p}$ (estimated using Equation 2) were applied to Equation 1 to calculate $Q_{\rm p}$ for the right and left sides. As in Seymour et al. (2015), η was assumed to be held constant at 0.04 dynes s/cm. Total $Q_{\rm p}$ is equal to the sum of the $Q_{\rm p}$ of the right and left sides, to account for the bilaterality of the ICAs.

 $M_{\rm b}$ values were calculated as averages of the male and female median (50% percentile) values from the 2000 CDC weight for age growth chart data tables (Kuczmarski et al., 2000). However, because the CDC growth charts end at age 20, $M_{\rm b}$ used to predict the "adult" $Q_{\rm p}$ was the mean of 21–39 years male and female averages from Dekaban and Sadowsky (1978). $M_{\rm b}$ values used to produce Equation 4 are reported in Supporting Information, Table S2, while $M_{\rm b}$ values used to generate $\tau_{\rm p}$ estimates using Equation 4 are reported in Table 2.

 $Q_{\rm ICA}$ and $r_{\rm ICA}$ were collected from the literature (Supporting Information, Tables S2 and S3). The $Q_{\rm ICA}$ and $r_{\rm ICA}$ used largely represent mean values reported in cross-sectional studies (Kehrer, Goelz, & Schöning,

2004; Scheel et al., 2000; Schöning & Hartig, 1996; Schöning & Hartig, 1998) with the exception of the measurements from Kehrer and Schöning (2009), which is a longitudinal study of one boy and one girl from 0 to 30 months old. For this longitudinal dataset, mean age, $Q_{\rm ICA}$ and $r_{\rm ICA}$ values were calculated for <1-, 1- to 2-, and >2-year-old time bins. Data in tables from Schöning and Hartig (1996) were summarized too coarsely, so data points were digitized from figures using WebPlotDigitizer (Rohatgi, 2018). From that dataset, age, $Q_{\rm ICA}$, and $r_{\rm ICA}$ values were binned in 1 year time intervals for individuals <18 years old, then each bin was averaged. The data digitized from the figures in Schöning and Hartig (1996, 1998) may be found in Supporting Information, Tables S2 and S3. "Adult" values represent mean values of individuals of 20–39 years old (Scheel et al., 2000). Total $Q_{\rm ICA}$ is equal to 2 × $Q_{\rm ICA}$.

Measured rate of brain perfusion and predicted rate of brain perfusion through the bilateral ICAs (in cm³/min/100 g) was calculated as (Total $Q_{\rm ICA}$ /brain mass \times 100) and (Total $Q_{\rm p}$ /brain mass \times 100), respectively. Brain masses were predicted for a given age (the middle of each age bin) using spline regression models fit by Kuzawa et al. (2014) to brain mass data published in Dekaban and Sadowsky (1978). Male and female brain masses calculated from this equation were averaged for a given age. Mass-specific rates of brain glucose utilization (BGU) were calculated by dividing male and female averaged brain glucose uptake (g/day) by male and female averaged brain glucose uptake (g/day) by male and female averaged brain mass (g) from Supporting Information, Tables S1 and S2 of Kuzawa et al. (2014).

Total $Q_{\rm ICA}$, Total $Q_{\rm p}$, measured and predicted rate of brain perfusion through the ICA, and mass-specific BGU rates were plotted against age and compared.

3 | RESULTS

Total flow measured through the ICAs (Total $Q_{\rm ICA}$) of human children increases rapidly from birth to 4–6 years old and appears to reach a maximum value between 5 and 6 years of age before decreasing with age at a slower pace (Figure 2a and Supporting Information, Table S2).

Total flow predicted for the ICAs (Total Q_p) shows a rapid increase in value from 0 to 5 years old and reaches a peak between 5 and 8 years of age (Figure 2a), with the maximal value of 12.36 mL/s at 8 years (Table 2). After peaking, Total $Q_{\rm p}$ decreases to as low as 7.22 mL/s at approximately age 16. The slope of the decrease in Total Qp with increasing age after reaching the maxima is steeper than in Total Q_{ICA} . In nearly every case, error bars representing 1 SD of the mean for Q_p and Q_{ICA} overlap extensively in similar age groups although Total Q_D values overall tend to be higher than Total Q_{ICA} for a given age, except for the age 16 estimate (Figure 2a). While both the measured and predicted flow rates peak during ontogeny and have a lower adult value, neither decline as dramatically as rates of whole brain glucose uptake (Figure 1a). Adult whole brain glucose uptake is about half of its ontogenetic peak, while we find that the measured and predicted adult ICA blood flow rates are about 87% and 76% of their ontogenetic peaks, respectively.

The rate of glucose uptake per gram of brain tissue increases with age from birth to year 5, before decreasing through the rest of the

TABLE 2 Predicted vessel lumen radii, predicted blood flow through the ICA, brain mass, body mass, and perfusion through the ICA

		Left			Right	Right								
Age	Year	n	r _p	Sd	n	r _p	Sd	$ au_p$	Tot Q _p	hi sd	lo sd	BrM	$M_{\rm b}$	PF_p
Newborn	80.0	7	1.07	0.20	7	1.08	0.17	39.0	1.92	3.1	1.1	411	3.7	28.0
2-3 months	0.25	8	1.06	0.20	8	1.05	0.19	38.3	1.77	2.9	1.0	522	5.8	20.3
4-10 months	0.625	10	1.46	0.17	11	1.45	0.19	37.4	4.56	6.5	3.1	726	8.2	37.7
1	1.5	6	1.73	0.24	6	1.62	0.21	36.4	6.73	9.8	4.4	1,009	11.3	40.0
2	2.5	13	1.77	0.19	13	1.76	0.29	35.7	7.72	11.3	5.0	1,139	13.2	40.7
3	3.5	10	1.87	0.25	10	1.88	0.17	35.1	9.09	12.5	6.4	1,202	15.0	45.4
4	4.5	14	1.94	0.21	14	1.93	0.22	34.3	9.78	13.4	6.9	1,235	17.1	47.5
5	5.5	12	2.02	0.19	12	2.04	0.18	33.6	11.05	14.3	8.3	1,248	19.3	53.1
6-7	7	8	2.07	0.13	8	2.03	0.19	32.3	10.90	13.6	8.6	1,259	23.0	52.0
8	8.5	6	2.14	0.22	5	2.20	0.29	30.8	12.36	17.3	8.5	1,287	27.2	57.6
9-11	10	7	2.09	0.25	7	2.09	0.32	28.2	10.15	14.9	6.5	1,326	34.6	45.9
15-17	16	6	2.14	0.27	5	2.05	0.18	19.9	7.22	9.8	5.2	1,368	58.5	31.7
Adults	30	57	2.36	0.26	52	2.35	0.04	18.1	9.35	11.3	7.8	1,380	63.5	40.7

Note. Age = age bins used by Lang et al. (1983); year = numerical year used for plotting in Figure 2a,c; n = number of individuals as reported in Lang et al. (1983); r_p = mean estimated ICA lumen radius (mm); sd = standard deviation of ICA lumen radius (mm), estimated from the foramen radius standard deviation; τ_p = ICA wall shear stress (dynes/cm²) predicted from Equation 4, used to calculate Q_p ; Tot Q_p = sum of left- and right-side predicted blood flow through the ICA (mL/s); hi sd = sum of right and left Q_p (mL/s) predicted using r_p + sd; lo sd = sum of right and left Q_p (mL/s) predicted using r_p - sd; BrM = brain mass (g); M_p = body mass in kg, used to predict τ_p using Equation 4; PF $_p$ = mass-specific predicted rate of brain perfusion through the ICA (mL/min/100 g brain tissue). Juvenile M_b are the means of male and female 50% percentile values from CDC weight to age growth charts data tables (https://www.cdc.gov/growthcharts/percentile_data_files.htm; Kuczmarski et al. 2000), averaged over the age bins defined by Lang et al. (1983). For example, the "age 3" bin M_b are averages of values from 36.5 to 47.5 months in the CDC weight to age data table. Newborn was interpreted to mean 0-1 month of age. Adult M_b is the male and female means for adults 20-39 years old in Dekaban and Sadowsky (1978), as the CDC charts end at age 20 years. BrM are the averages of male and female values calculated for a given year using predictive equations from Kuzawa et al. (2014).

juvenile period into adulthood (Figure 2b). Brain mass-specific *Q* (perfusion) increases and reaches a maximum at age 5 before decreasing in measured values, but reaches a maximum at age 8 for predicted values (Figure 2c, Supporting Information, Figure S2, Table 2, and Supporting Information, Table S2).

4 | DISCUSSION

Prior work using clinical data has shown that a number of different measures including (a) brain glucose uptake as a % of RMR (Kuzawa et al., 2014), (b) the fraction of total cardiac output accounted for by the brain (Wu et al., 2016), and (c) oxygen-based measures of cerebral metabolism (Goyal, Hawrylycz, Miller, Snyder, & Raichle, 2014) all follow similar developmental patterns characterized by a rapid early postnatal rise to a mid-childhood peak, followed by a decline to adult values across the adolescent years. Using carotid foramen radii, estimates of vessel wall shear stress, and the modified Poiseuille-Hagan equation, we find that predicted rates of ICA blood flow (Qp) adhere well to direct measures of ICA blood flow (Q_{ICA}) during childhood, and that these measures closely correspond to known developmental changes in human brain metabolism. Thus, our findings suggest that blood flow and perfusion predicted from skeletal measures of ICA size may be a useful tool for probing the developmental timing and magnitude of energetic costs, and related tradeoffs with bodily expenditures like growth, of the developing brain.

Although these findings point to the promise of this method for reconstructing developmental changes in brain metabolism, estimates of flow rates and perfusion obtained from osteological measures using this method should be interpreted with caution. There are several potential sources of error, particularly if the method is applied to new

samples. According to the Poiseuille-Hagan equation (Equation 1), flow rate Q is related to vessel radius r to the third power, which means that errors associated with estimating lumen radius r_p from foramen radii impact blood flow rate predictions Q_p more profoundly than other variables in the model. For example, although the adult value of Q_p obtained by this study (9.4 mL/s) closely matches measured adult Q_{ICA} (9.2 mL/s), this finding may be a coincidence, given a probable inaccuracy in the carotid foramen radii that we used to predict Q_p. Specifically, our source of measurements of carotid foramen diameters (Lang et al., 1983), neglected to report minimum diameters for adults of their sample. This could lead to an overestimate of r_p (and hence Q_p) for adults. Data from other studies also indicate that the diameters presented by the Lang et al. (1983) study and flow rates calculated with their data may be slightly inflated. For example, Seymour et al. (2015) report a mean r_p of 2.19 mm from a sample of n = 7 adult crania, which yields a Total Q_p predicton of only 7.5 mL/s. A study by Çalgüner et al. (1997) suggest that mean adult carotid foramen radii may be as low as 2.79 mm in their study population, which would yield an r_p of 2.0 mm and Total Q_p of only 5.7 mL/s. Because τ_{ICA} (calculated from adult measured Q_{ICA} : 18.11 dynes/cm²) is similar to τ_p (predicted using Equation 4 to calculate predicted flow, Q_p: 18.14 dynes/cm²), shear stress prediction is not what is driving the difference in these Q_p values.

The high jump in mean value for Q_p and predicted rate of brain perfusion at age 8 is due to the mean carotid foramen diameter measurement for that age group being larger than those in the age bins immediately preceding (6–7 years) and succeeding (9–11 years) it (Supporting Information, Table S1). Confidence in the 8-year-old value is, however, lower because its sample size of carotid foramina measurements is low (n = 6 for left and n = 5 for right) relative to several

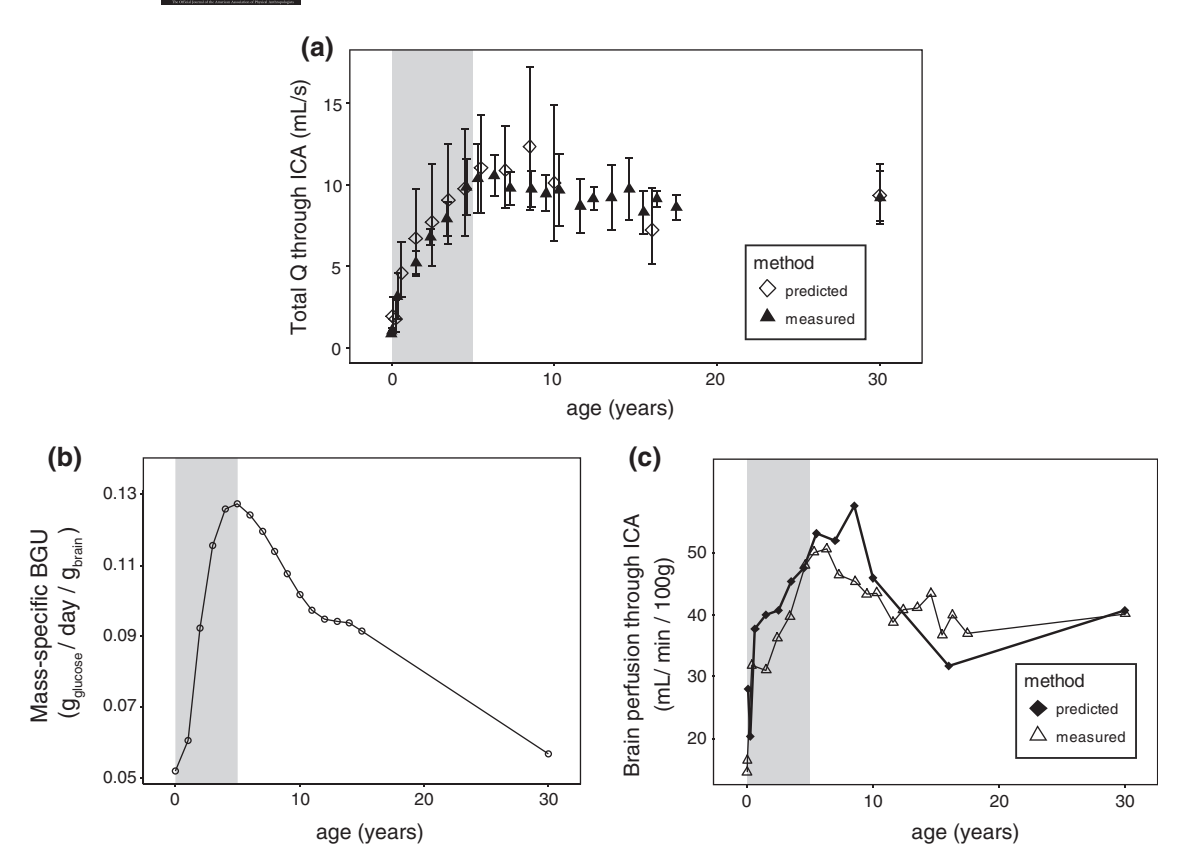


FIGURE 2 (a) Pattern of change in total predicted blood flow through the left and right internal carotid arteries (ICAs) match observed patterns of change in total measured ICA blood flow; mean predicted values typically fall within one standard deviation of measured values. (b) Brain glucose uptake (BGU) relative to brain mass peaks around age 5 before declining, as do (c) measured rates of brain perfusion through the ICAs, indicating a match in the timing of highest brain mass-specific brain metabolism and measured blood flow. Predicted rates of brain perfusion are highest between ages 5 and 8, roughly matching the timing of highest mass-specific brain metabolism. Gray shaded box represents values in in the 0–5 years age range. Measured blood flow rates data are in Supporting Information, Table S2; predicted blood flow rates data are in Table 2; BGU and brain masses are from Kuzawa et al. (2014). Error bars in (a) represent one standard deviation from the mean

close age bins (n = 12 for age 5; n = 8 for age 6–7; n = 7 for age 9–11). Thus, the finding that peak in predicted values occurs at 8 years instead of 5 years as for measured values could simply be the result of a biased sample of five larger than average 8-year-olds.

Furthermore, to the best of our knowledge, it is currently unknown how variable carotid foramen sizes are at different ages between populations or within populations, or even between males and females at a particular age. Lang et al. (1983) do not divide their sample by sex and do not elaborate on the sample population, complicating assessment of these issues. In addition, our analysis is somewhat limited by the coarseness of age bins summarized by Lang et al. (1983), particularly in the older age groups (beyond year 5), where the sample size for each age bin also tends to be smaller than the younger age categories (Table 2). In future tests, use of additional, more age-refined samples of skulls with associated recording of biological variables, such as sex and body mass, may reveal smoother and more consistent patterns of change in carotid foramen radius and $Q_{\rm p}$ with age.

Another potential source of error in the accuracy of the predicted blood flow rates is artery wall shear stress. As far as we are aware, there are no studies that report empirically measured ICA wall shear stress through human ontogeny with which to compare the τ_{ICA} estimates obtained in this study. It is also unclear whether the scaling relationship of τ_{ICA} with body mass that we derived (Equation 4) is the best

method for predicting τ_p for calculation of Q_p in this sample. Allometric analysis suggests that wall shear stress is lower as body mass increases (Weinberg & Ethier, 2007). However, Samijo et al. (1998) show that wall shear stress of the common carotid arteries decreases with age in adult humans. They suggest that this phenomenon is related to the increase in common carotid artery radius with age. Once reaching adulthood, there is no reason to assume that aging is associated with a systematic increase in mass, as is the case during growth. Although body mass was used for modeling τ_{ICA} because we wanted to map how flow rates change with age, it is possible that age is a more appropriate predictor of vessel wall shear stress in this intraspecific sample.

Despite these potential sources of error, the method used here was generally successful in generating blood flow and perfusion estimates that mirror ontogenetic patterns reported in previous studies using direct physiological and metabolic measurements. Although the timing of maximum $Q_{\rm p}$ (8 years) does not exactly match the ages for maxima in BGU published previously, or $Q_{\rm ICA}$ in children (5–6 years) in the current sample, the findings of this study demonstrate that the modified Poiseuille–Hagan equation, combined with reasonably reliable estimates of wall shear stress and ICA lumen radius, captures general patterns of change that mirror predicted changes in measured flow rates, and may be useful in the prediction of developmental changes in ICA blood flow rates during human ontogeny.

The correspondence of predicted and measured ICA blood flow rates in this human sample also shows promise in its potential to accurately predict blood flow rates to the brain for other interspecific and intraspecific samples. Unfortunately, verifying the accuracy of shear stress estimates, lumen radii, and Q_p will likely be difficult when the approach is applied to new taxonomic samples because known values from empirical measurements are scarce or nonexistent in most cases. Therefore, for many osteological samples, and always for fossil ones, these unknown parameters will have to be inferred from extant samples in which the data are available (as has previously been done in the studies of Seymour et al., 2015, 2016, and Boyer & Harrington, in press). Despite these limitations, we believe that the method may be particularly useful for predicting relative variation in ICA blood flow rates within species where necessary assumptions about which variables are constant are potentially more robust. For example, the proportion of the carotid foramen occupied by the ICA may be less variable within a species than between species, and the Poiseuille-Hagan equation again would predict that estimated lumen radius would be a proportionally greater determinant of flow rate than vessel wall shear stress. Thus, in intraspecific ontogenetic comparisons, observations of changes in the size of the carotid foramen relative to brain size may themselves be useful for making basic inferences about relative blood flow rates.

One potential future application is to the hominin fossil record, where this method may be a useful tool for describing the timing of the evolutionary emergence of a suite of modern human life history traits that likely co-evolved with our energy-intensive form of brain growth and development. Specifically, comparisons of the developmental timing of greatest cerebral blood flow (and hence brain metabolism) could allow inference of whether fossil hominin species had a modern human-like pattern of energy-intensive brain development. As fossil samples of varying developmental ages accrue for a taxon, this could provide insights into age-specific patterns of predicted brain perfusion. By extension, such data could be informative about whether metabolically expensive processes related to cognitive development, such as high synaptic densities, may have occurred with similar timing, magnitude, and duration in fossil hominin species when compared to modern humans.

It should be cautioned, however, that the use of Q_p as a correlate to the metabolic rate of the brain-or even just the cerebrum, of which the ICA typically supplies many parts (Gillilan, 1972; Tatu et al., 1998)—may not be equally applicable across all species. One potential confounding variable is the role of arterial flow in the thermoregulation of the brain. It has previously been hypothesized that variation in the size and pattern of vasculature in and around the brain observed in fossil hominin and human endocasts and crania may be related to thermoregulatory adaptations as humans evolved in heat-stressed environments (Falk, 1986; Falk, 1990). Indeed, because the human brain is too large to effectively lose heat to the environment via conduction through the scalp, temperature homeostasis in the human brain is largely maintained by convective heat exchange with arterial blood flow (Brengelmann, 1993; Kauppinen, Vidyasagar, Childs, Balanos, & Hiltunen, 2008; Wang et al., 2014). However, changes in brain tissue temperature are associated with localized blood flow in smalldiameter arterioles, where the heat equilibrium can be achieved most effectively (Hayward & Baker, 1968; Kauppinen et al., 2008). Flow rate in large encephalic vessels such as the ICA has been reported to be relatively stable under normal circumstances, even during "moderate" exercise, although hypothermia and "intense" exercise have been linked to lower total cerebral blood flow (Nybo & Secher, 2004; Nybo, Secher, & Nielsen, 2002; Wang et al., 2014). Given this information, it appears that ICA blood flow rate would not be expected to fluctuate with downstream thermoregulatory functions caused by metabolic activity under normal conditions. This certainly does not rule out a relationship between ICA flow rate and the brain's thermoregulatory needs: because much of the heat balance of the brain is affected by its metabolic activity, it will be difficult to decouple the effect of brain metabolism from heat homeostasis on regional and global brain blood flow rates.

Furthermore, although changes in Q_{ICA} by age correspond to age changes in BGU in humans (and sheep fetuses: Van Bel et al. 1994), Boyer and Harrington (2018a, in press) provide evidence that the proportion of blood to the brain supplied by the ICAs relative to that supplied by the vertebral arteries is not constant across species. This variation may result from differences in the sizes, mass-specific metabolism, and regions of supply by the ICAs and vertebral arteries within the brain. However, it may also result if significant ICA or vertebral artery flow volumes supply structures outside of the brain. For example, the degree to which the orbit and eyeball is supplied by ophthalmic branches of the ICA varies among primates (Bugge, 1974), and there is evidence that the anterior portion of the meninges may be regularly supplied by ophthalmic branches in nonhuman apes (Falk, 1993). Although we suspect that the proportion of ICA blood flow that supplies nonbrain structures is relatively low, this possible confounding factor merits further investigation.

Lastly, even within a species, the relative contributions of the ICAs and vertebral arteries to brain perfusion may shift ontogenetically. In fact, Schöning and Hartig (1996) noted that roughly 31% of the human brain's total blood flow volume is carried by the vertebral arteries in young children, whereas they contribute 24% of brain blood flow volume in adults. This difference in relative contribution by the vertebral arteries to total brain blood flow with age may also explain why the reduction in measured ICA blood flow rate in adulthood from the childhood peak is not as great as the difference seen in BGU. Based on this, we speculate that future work combining data on flow from the vertebral artery with the ICA will yield a pattern of ontogenetic changes in blood flow that more closely matches brain glucose uptake than the changes that we report here based solely on ICA blood flow. This interpretation gains initial support from graphical evidence presented in Schöning and Hartig (1996) and Wu et al. (2016), which suggest that total blood flow (inclusive of blood flow through the vertebral arteries and ICAs) to the brain in adults is around 75% (or less) of childhood peak values. In contrast, in this study, measured and predicted adult ICA blood flow values were between 75% and 90% of the childhood maximum. Therefore, adapting the methodology described here for prediction of Q for the vertebral arteries and accounting for their additional contribution to encephalic blood flow will be an important refinement for studies aimed at reconstructing fossil proxies of total cerebral blood flow and metabolism.

In sum, we show that the blood flow rates predicted from the carotid foramen are well matched to flow rates of the ICAs during much of infancy and childhood, which in turn are roughly similar to patterns of change in mass-specific and whole brain metabolism. Therefore, this study provides evidence that arterial lumen and canal size directly tracks the brain's shifting burden on the body's energy budget during human growth and development, and indicates the potential utility of this approach for exploring these relationships in fossil hominins.

ACKNOWLEDGMENTS

We thank an anonymous reviewer for their helpful comments and thank our funding sources NSF BCS 1552848 (to D. Boyer), NSF DBI 1701714 (to D. Boyer), and NSF BCS 1825129 (to D. Boyer and A. Harrington).

ORCID

Arianna R. Harrington https://orcid.org/0000-0002-2720-6098

REFERENCES

- Aiello, L. C., & Wheeler, P. (1995). The expensive-tissue hypothesis: The brain and the digestive system in human and primate evolution. *Current Anthropology*, 36(2), 199–221.
- Armstrong, E. (1983). Relative brain size and metabolism in mammals. *Science*, 220(4603), 1302–1304.
- Boyer, D. M., & Harrington, A. R. (2018a). Scaling of bony canals for encephalic vessels in euarchontans: Implications for the role of the vertebral artery and brain metabolism. *Journal of Human Evolution*. 114, 85–101.
- Boyer, D. M., & Harrington, A. R. (in press). New estimates of blood flow rates in the vertebral artery of Euarchontans and their implications for encephalic blood flow scaling: A response to Seymour and Snelling (2018). *Journal of Human Evolution*. https://doi.org/10.1016/j. jhevol.2018.10.002
- Brengelmann, G. L. (1993). Specialized brain cooling in humans? *The FASEB Journal*, 7(12), 1148–1152.
- Bugge, J. (1974). The cephalic arterial system in insectivores, primates, rodents, and lagomorphs, with special reference to the systematic classification. *Acta Anatomica*, 87, (1–160).
- Çalgüner, E., Turgut, H., Gözil, R., Tunç, E., Sevim, A., & Keskil, S. (1997). Measurements of the carotid canal in skulls from Anatolia. *Cells, Tissues, Organs*, 158(2), 130–132.
- Cebral, J., Castro, M., Putman, C., & Alperin, N. (2008). Flow-area relationship in internal carotid and vertebral arteries. *Physiological Measure*ment, 29(5), 585-594.
- Cheng, C., Helderman, F., Tempel, D., Segers, D., Hierck, B., Poelmann, R., ... Ursem, N. T. (2007). Large variations in absolute wall shear stress levels within one species and between species. Atherosclerosis, 195(2), 225–235.
- Chugani, H. T., Phelps, M. E., & Mazziotta, J. C. (1987). Positron emission tomography study of human brain functional development. *Annals of Neurology*, 22(4), 487–497.
- Coceani, F., & Gloor, P. (1966). The distribution of the internal carotid circulation in the brain of the macaque monkey (Macaca mulatta). Journal of Comparative Neurology, 128(4), 419–429.
- de León, M. S. P., Golovanova, L., Doronichev, V., Romanova, G., Akazawa, T., Kondo, O., ... Zollikofer, C. P. (2008). Neanderthal brain size at birth provides insights into the evolution of human life history. Proceedings of the National Academy of Sciences of the United States of America, 105(37), 13764–13768.
- Dekaban, A. S., & Sadowsky, D. (1978). Changes in brain weights during the span of human life: Relation of brain weights to body heights and body weights. *Annals of Neurology*, 4(4), 345–356.
- Falk, D. (1986). Evolution of cranial blood drainage in hominids: Enlarged occipital/marginal sinuses and emissary foramina. American Journal of Physical Anthropology, 70(3), 311–324.

- Falk, D. (1990). Brain evolution in Homo: The "radiator" theory. Behavioral and Brain Sciences. 13(2), 333–344.
- Falk, D. (1993). Meningeal arterial patterns in great apes: Implications for hominid vascular evolution. American Journal of Physical Anthropology, 92(1), 81–97.
- Foley, R. A., & Lee, P. C. (1991). Ecology and energetics of encephalization in hominid evolution. *Philosophical transactions of the Royal Society of London. Series B*, 334(1270), 223–232.
- Gillilan, L. A. (1972). Blood supply to primitive mammalian brains. *Journal of Comparative Neurology*, 145(2), 209–221.
- Goyal, M. S., Hawrylycz, M., Miller, J. A., Snyder, A. Z., & Raichle, M. E. (2014). Aerobic glycolysis in the human brain is associated with development and neotenous gene expression. *Cell Metabolism*, 19 (1), 49–57.
- Greve, J. M., Les, A. S., Tang, B. T., Draney Blomme, M. T., Wilson, N. M., Dalman, R. L., ... Taylor, C. A. (2006). Allometric scaling of wall shear stress from mice to humans: Quantification using cine phase-contrast MRI and computational fluid dynamics. *American Journal of Physiology*. *Heart and Circulatory Physiology*, 291(4), H1700–H1708.
- Hawkins, R. A., Mans, A. M., Davis, D. W., Hibbard, L. S., & Lu, D. M. (1983). Glucose availability to individual cerebral structures is correlated to glucose metabolism. *Journal of Neurochemistry*, 40(4), 1013–1018.
- Hayward, J. N., & Baker, M. A. (1968). Role of cerebral arterial blood in the regulation of brain temperature in the monkey. American Journal of Physiology-Legacy Content, 215(2), 389–403.
- Hofman, M. A. (1983). Energy metabolism, brain size and longevity in mammals. *The Quarterly Review of Biology*, 58(4), 495–512.
- Isler, K., & van Schaik, C. P. (2006). Metabolic costs of brain size evolution. Biology Letters, 2(4), 557–560.
- Isler, K., & van Schaik, C. P. (2009). The expensive brain: A framework for explaining evolutionary changes in brain size. *Journal of Human Evolution*, 57(4), 392–400.
- Karbowski, J. (2007). Global and regional brain metabolic scaling and its functional consequences. *BMC Biology*, *5*(1), 18.
- Kauppinen, R. A., Vidyasagar, R., Childs, C., Balanos, G. M., & Hiltunen, Y. (2008). Assessment of human brain temperature by 1H MRS during visual stimulation and hypercapnia. NMR in Biomedicine, 21(4), 388–395.
- Kehrer, M., Goelz, R., & Schöning, M. (2004). The development of haemodynamics in the extracranial cerebral arteries of healthy preterm and term neonates. *Ultrasound in Medicine and Biology*, 30(3), 283–287.
- Kehrer, M., & Schöning, M. (2009). A longitudinal study of cerebral blood flow over the first 30 months. *Pediatric Research*, 66(5), 560–564.
- Kuczmarski, R., Ogden, C., Grummer-Strawn, L., Flegal, K., Guo, S., Wei, R., ... Johnson, C. (2000). CDC growth charts: United States. Advance data, (314), 1–28.
- Kuzawa, C. W. (1998). Adipose tissue in human infancy and childhood: An evolutionary perspective. American Journal of Physical Anthropology, 107(527), 177–209.
- Kuzawa, C. W., Chugani, H. T., Grossman, L. I., Lipovich, L., Muzik, O., Hof, P. R., ... Lange, N. (2014). Metabolic costs and evolutionary implications of human brain development. Proceedings of the National Academy of Sciences of the United States of America. 111(36), 13010–13015.
- Lang, J., Schafhauser, O., & Hoffmann, S. (1983). Postnatal development of transbasal skull openings: Carotid canal, jugular foramen, hypoglossal canal, condylar canal and foramen magnum. *Anatomischer Anzeiger*, 153 (4), 315–357.
- Leonard, W. R., & Robertson, M. L. (1992). Nutritional requirements and human evolution: A bioenergetics model. *American Journal of Human Biology*, 4(2), 179–195.
- Lou, H. C., Edvinsson, L., & MacKenzie, E. T. (1987). The concept of coupling blood flow to brain function: Revision required? *Annals of Neurol*ogy, 22(3), 289–297.
- Martin, R. D. (1981). Relative brain size and basal metabolic rate in terrestrial vertebrates. *Nature*, 293(5827), 57–60.
- McNab, B. K., & Eisenberg, J. F. (1989). Brain size and its relation to the rate of metabolism in mammals. The American Naturalist, 133(2), 157–167
- Nybo, L., & Secher, N. H. (2004). Cerebral perturbations provoked by prolonged exercise. *Progress in Neurobiology*, 72(4), 223–261.

- Nybo, L., Secher, N. H., & Nielsen, B. (2002). Inadequate heat release from the human brain during prolonged exercise with hyperthermia. *The Journal of Physiology*, 545(2), 697–704.
- Rohatgi A. 2018. WebPlotDigitizer (Version 4.1).
- Samijo, S., Willigers, J., Barkhuysen, R., Kitslaar, P., Reneman, R., Brands, P., & Hoeks, A. (1998). Wall shear stress in the human common carotid artery as function of age and gender. *Cardiovascular Research*, 39(2), 515–522.
- Scheel, P., Ruge, C., & Schöning, M. (2000). Flow velocity and flow volume measurements in the extracranial carotid and vertebral arteries in healthy adults: Reference data and the effects of age. *Ultrasound in Medicine and Biology*, 26(8), 1261–1266.
- Schöning, M., & Hartig, B. (1996). Age dependence of total cerebral blood flow volume from childhood to adulthood. *Journal of Cerebral Blood Flow & Metabolism*, 16(5), 827–833.
- Schöning, M., & Hartig, B. (1998). The development of hemodynamics in the extracranial carotid and vertebral arteries. *Ultrasound in Medicine and Biology*, 24(5), 655–662.
- Seymour, R. S., Angove, S. E., Snelling, E. P., & Cassey, P. (2015). Scaling of cerebral blood perfusion in primates and marsupials. *The Journal of Experimental Biology*. 218(Pt 16), 2631–2640.
- Seymour, R. S., Bosiocic, V., & Snelling, E. P. (2016). Fossil skulls reveal that blood flow rate to the brain increased faster than brain volume during human evolution. *Royal Society Open Science*, *3*(8), 160305.
- Seymour, R. S., Bosiocic, V., & Snelling, E. P. (2017). Correction to 'Fossil skulls reveal that blood flow rate to the brain increased faster than brain volume during human evolution'. *Royal Society Open Science*. 4, 170846.
- Tatu, L., Moulin, T., Bogousslavsky, J., & Duvernoy, H. (1996). Arterial territories of the human brain: Brain stem and cerebellum. *Neurology*, 47, 1125–1135.
- Tatu, L., Moulin, T., Bogousslavsky, J., & Duvernoy, H. (1998). Arterial territories of the human brain cerebral hemispheres. *Neurology*, 50(6), 1699–1708.
- Van Bel, F., Roman, C., Klautz, R.J., Teitel, D.F., & Rudolph, A. M. (1994). Relationship between brain blood flow and carotid arterial flow in the sheep fetus. *Pediatric research*, 35(3), 329.

- Walker, R., Hill, K., Burger, O., & Hurtado, A. M. (2006). Life in the slow lane revisited: Ontogenetic separation between chimpanzees and humans. American Journal of Physical Anthropology, 129(4), 577–583.
- Wang, H., Wang, B., Normoyle, K. P., Jackson, K., Spitler, K., Sharrock, M. F., ... Du, R. (2014). Brain temperature and its fundamental properties: A review for clinical neuroscientists. Frontiers in Neuroscience, 8, 307.
- Weinberg, P. D., & Ethier, C. R. (2007). Twenty-fold difference in hemodynamic wall shear stress between murine and human aortas. *Journal of Biomechanics*, 40(7), 1594–1598.
- Willie, C. K., Tzeng, Y. C., Fisher, J. A., & Ainslie, P. N. (2014). Integrative regulation of human brain blood flow. *The Journal of Physiology*, 592(5), 841–859
- Wu, C., Honarmand, A. R., Schnell, S., Kuhn, R., Schoeneman, S. E., Ansari, S. A., ... Shaibani, A. (2016). Age-related changes of normal cerebral and cardiac blood flow in children and adults aged 7 months to 61 years. *Journal of the American Heart Association*, 5(1), e002657.
- Wu, S. P., Ringgaard, S., Oyre, S., Hansen, M. S., Rasmus, S., & Pedersen, E. M. (2004). Wall shear rates differ between the normal carotid, femoral, and brachial arteries: An in vivo MRI study. *Journal of Magnetic Resonance Imaging*, 19(2), 188–193.

SUPPORTING INFORMATION

Additional supporting information may be found online in the Supporting Information section at the end of this article.

How to cite this article: Harrington AR, Kuzawa CW, Boyer DM. Carotid foramen size in the human skull tracks developmental changes in cerebral blood flow and brain metabolism. *Am J Phys Anthropol.* 2019;169:161–169. https://doi.org/10.1002/ajpa.23809